Tectonophysics 800 (2021) 228705

Contents lists available at ScienceDirect

Tectonophysics

journal homepage: www.elsevier.com/locate/tecto

Structural signatures of the Amazonian Craton in eastern Colombia from gravity and magnetometry data interpretation

Ismael Enrique Moyano Nieto [a,b,*], German A. Prieto [a]

[a] Departamento de Geociencias, Universidad Nacional de Colombia, Bogotá, Colombia
[b] Servicio Geológico Colombiano, Dirección de Recursos Minerales, Diagonal 53, 34-53 Bogotá, Colombia

ARTICLE INFO

Keywords:
Magnetic/gravity data interpretation
Multiscale edge detection
NW Amazonian Craton
Structural interpretation

ABSTRACT

Geophysical interpretation of potential field data plays an important role in the integration of geological data. Estimation of density and magnetic susceptibility variations within the upper crust helps evaluating the continuity of geological structures in the field. In the present study we use gravity and magnetic data in NW Amazonian Craton in Colombia. Total horizontal gradient of the reduction to magnetic pole were used to delineate magnetic lineaments and domains showing four zones, each with its own features. Multiscale edge detection (worming) of the data help delineate upper crustal structures that we interpret as tectonic boundaries that correlate with the four zones identified. 3D density and magnetic susceptibility inversion showed high density and/or high magnetic susceptibility sources correlated with these crustal structures. Zone (1) is located south of the Guaviare River, with predominant NW-SE and NE-SW magnetic lineaments; zone (2), located from south of the Guaviare River to the north, present nearly *E*-W magnetic lineaments and a deep E-W edge interpreted as a possible shear zone parallel to Guaviare, Orinoco and Ventuari rivers; zone (3) from south of the Vichada River to the north, with NE-SW and NW-SE lineaments; N-S zone (4) cuts the zones (2) and (3), characterized by high density/magnetic susceptibility source bounded by N-S deep edges. A more complete tectonic evolution interpretation requires further work, but we speculate that the zone (4) could indicate an aborted rift/collision suture and that the zone (2) is indicative of a younger deformation event. Shear direction at (2) is not clear: geological maps show NEE-SWW right-lateral faulting, but geophysical anomalies suggest left-lateral displacement, highlighted by left dislocation of the Orinoco River. We also speculate that a N-S edge located at the SE of the area can be related with the Atabapo Belt and the limit of Ventuari-Tapajós and Rionegro geochronological provinces.

1. Introduction

Geoscientific research of the Amazonian Craton in Colombia involves great challenges, not only due to its extent (nearly the 50% of the continental area of the country) and geological complexity, but also because most of the crystalline rocks that compose it are covered by sedimentary rocks and recent deposits (Gómez et al., 2015a; Gómez et al., 2015b; De la Espriella et al., 1990; González et al., 2014; Alfonso et al., 2014; Ochoa et al., 2014). In addition, dense vegetation coverage makes it difficult to access and identify outcrops of cratonic rocks, making this area one of the least geologically known areas in the world (Santos et al., 2000). Consequently, geological maps and models of the Amazonian craton in Colombia are mostly based on the integration of rock exposures at the east of the country, Brazil and Venezuela, and from isolated exposures within the sedimentary coverage (Galvis et al., 1979; Bruneton et al., 1983; López et al., 2010; Ochoa et al., 2014).

Colombia is located at the NW portion of the Guiana Shield (Fig. 1), that corresponds to the northern half of the Amazonian Craton (Santos et al., 2000; Brito, 2011; Ibáñez-Mejía et al., 2011; Kroonemberg, 2019; Cediel, 2019). The Guiana Shield is considered the backstop for the progressive accretion and continental growth of NW South America from Middle to Upper Proterozoic through to the Holocene (Cediel, 2019). Rocks of the Guiana shield are exposed in eastern Amazonia and eastern Llanos in Colombia, being progressively covered by younger sediments (Ordovician to Cenozoic Age) westwards to the Andes and southwards to the Amazon River (Kroonemberg, 2019).

Geological and geochronological models for the Amazonian Craton (Fig. 2) propose that the craton evolved from an ancient nucleus with

* Corresponding author at: Servicio Geológico Colombiano, Bogotá, Colombia.
E-mail addresses: iemoyanon@unal.edu.co, imoyano@sgc.gov.co (I.E. Moyano Nieto).

https://doi.org/10.1016/j.tecto.2020.228705
Received 15 October 2020; Received in revised form 7 December 2020; Accepted 15 December 2020
Available online 11 January 2021

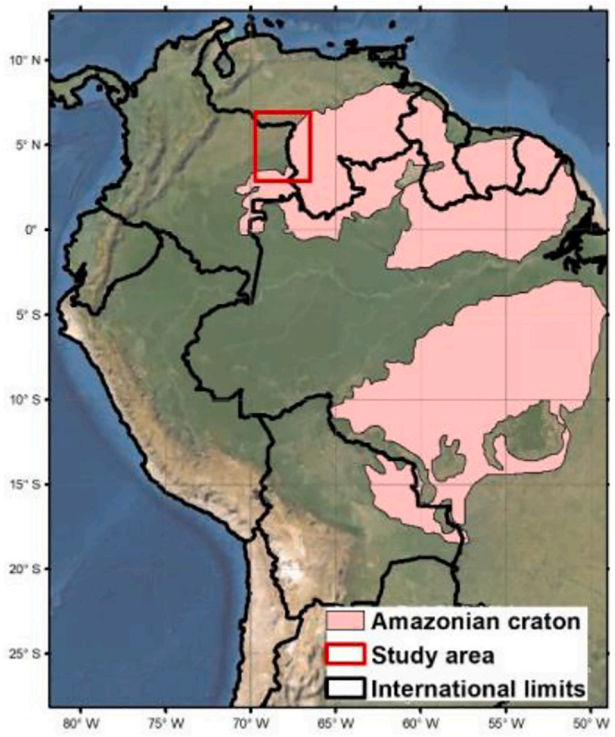

Fig. 1. Location of the study area and extension of the Amazonian Craton. Modified from Cordani et al., 2016a.

episodic lateral accretion of belts and/or terranes (Barrios et al., 1985; Tassinari and Macambira, 1999; Santos et al., 2000; Brito, 2011; Ibáñez-Mejía et al., 2011; Kroonemberg, 2019). Different tectonic/geochronological provinces or domains were delimited by the predominance of a characteristic geochronological pattern and coherence of the ages of different geological units (Tassinari and Macambira, 1999). Other models also integrate data from new geochronological methods and recent geological mapping, mainly in Brazil and Guiana (Santos et al., 2000; Kroonemberg, 2019). Geographic boundaries between provinces complement the geochronological data with some geological and geophysical control, but there is still debate on the exact boundaries because of inconsistency (Jackson, 1972; Parker, 1977; VanDecar and Snieder, 1994) in age determinations (e.g., two similar samples give different age) or the lack of reliable geological information (Tassinari and Macambira, 1999).

The basement of the Amazonian Craton in Colombia (Fig. 3) is formed by Paleoproterozoic granitoids and granitic gneisses identified Mitú Migmatitic complex (Gómez et al., 2015b; Galvis et al., 1979) or Mitú Complex (Celada et al., 2006; Rodríguez et al., 2010; López et al., 2010; Bonilla et al., 2016) or Cuchivero Group in Venezuela (Hackley et al., 2005). Basement rocks were intruded by Late Proterozoic syntectonic granites and Mesoproterozoic anorogenic granites (Kroonemberg, 2019). The most extensive anorogenic intrusive is the Middle Proterozoic Parguaza Rapakiwi Granite (Hackley et al., 2005). In Colombia, the Parguaza Granite exposures are limited to the left margin of the Orinoco River and isolated hills surrounded by recent deposits. Also, other Parguaza-like bodies were identified to the south, intruded within rocks of the Mitú Complex (Bruneton et al., 1983; De la Espriella et al., 1990; Bonilla et al., 2016). The Mitú Complex is also covered by low-grade metamorphosed and non-metamorphic sandstone plateaus and intruded by small Neoproterozoic basic and alkaline intrusions (Kroonemberg, 2019).

In this contribution we identify and delineate major structural and tectonic features within the crystalline rocks of the Amazonian Craton by modelling and interpretation of geophysical (gravity and magnetic) data. We integrate this new data with geological information to help improve the current structural/tectonic models for this area.

2. Geological setting

The study area corresponds to nearly 160.000 km^2 of eastern Colombia/western Venezuela (Fig. 3). Available geological maps for the whole area have a 1:500.000 scale for Colombia (Gómez et al., 2015b)

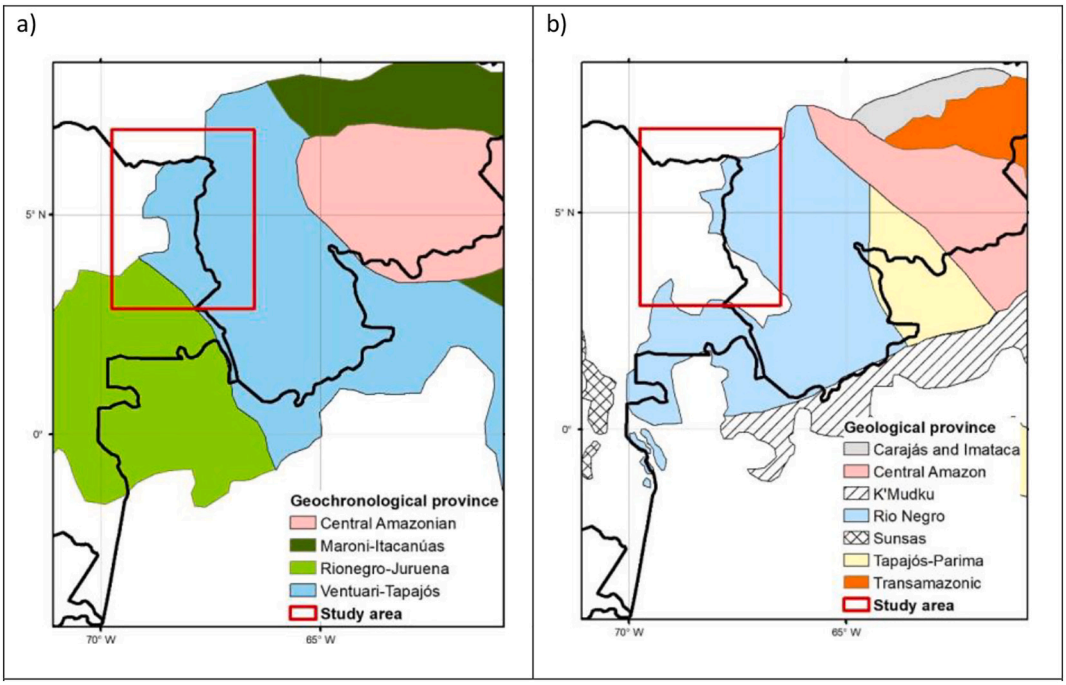

Fig. 2. Geochronological (a) and geological provinces (b) of the Amazonian Craton. Modified from Tassinari and Macambira, 1999 and Santos et al., 2000, respectively.

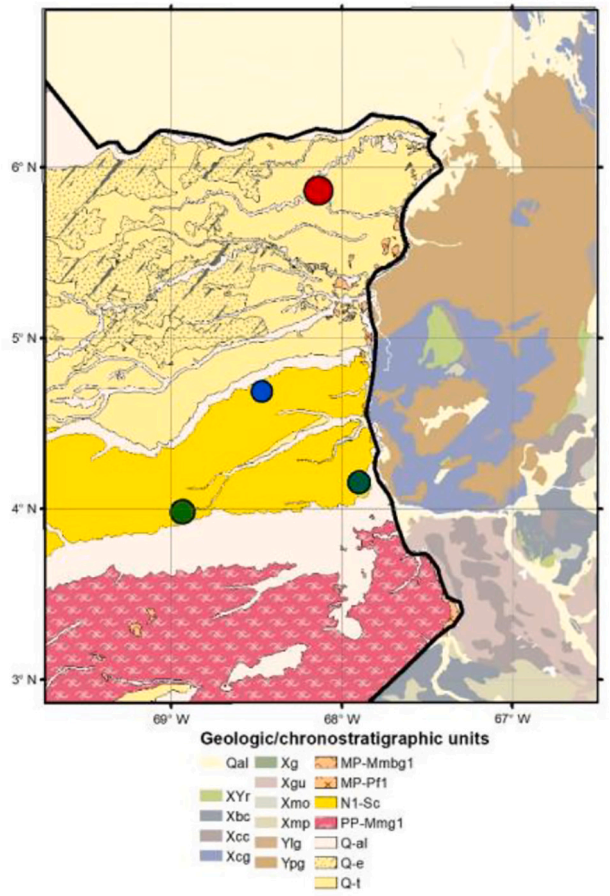

Fig. 3. Regional geology (modified from Gómez et al., 2015b and Hackley et al., 1995). Red dot: Cerro El Carajo metasandstones (Ochoa et al., 2012). Blue dot: westernmost exposure of Parguaza Granite (Alfonso et al., 2014). Green dots: northernmost exposure of Mitú Complex (López et al., 2010; Alfonso et al., 2014). See Table 1 for detailed description of each unit. (For interpretation of the references to colour in this figure legend, the reader is referred to the web version of this article.)

and 1:750.000 scale for Venezuela (Hackley et al., 2005). In approximately 70% of the study area, the Amazon Craton is covered by Cenozoic sedimentary deposits.

Crystalline basement is exposed in the southern region of Fig. 3 and to the east in Venezuela. general characteristics of the geological units presented in Fig. 3 are summarized in Table 1.

Geological maps from other projects (Galvis et al., 1979; Bruneton et al., 1983; De la Espriella et al., 1990) and 1:100.000 scale geological maps of the Servicio Geológico Colombiano (Cardozo et al., 2009; López et al., 2010; Ochoa et al., 2012; González et al., 2014; Alfonso et al., 2014; Ochoa et al., 2014) provide additional information like the identification of rocks related to the Mitú Complex further north of the actual maps (green dots, Fig. 3) (López et al., 2010; Alfonso et al., 2014). Also, location of Parguaza type granites 70 km westward from the Orinoco River (blue dot, Fig. 3; Alfonso et al., 2014) and the identification of the Neoproterozoic(?) "Cerro El Carajo" metasandstones (red dot, Fig. 3) (De la Espriella et al., 1990; González and Pinto, 1990; Ochoa et al., 2012).

2.1. Geochronology and geotectonic framework

The area corresponds to the geochronological provinces of Ventuari-Tapajós (VTP) and Rionegro-Juruena (RNJ, Fig. 2a) (Tassinari and Macambira, 1999) or the geological province of Rio negro (Fig. 2b) (Santos et al., 2000). Geochronological provinces are defined as major

Table 1
Description of the geological/geochronological units for the study area (Fig. 3).

Name/code	Age	Lithologies
Mitú Complex PP-Mmg1	Paleoproterozoic	Plagioclase feldspar gneisses, amphibolite, migmatites, quartzites, quartz-gneiss and granites with variations to alaskytes and monzonites;
Xbc Basement Complex	Early Proterozoic	Granite to granodiorite gneiss;
Xcg Cuchivero group	Early Proterozoic	Silicic intrusive rocks
Xmp San Carlos metamorphic-plutonic terrane	Early Proterozoic	Granite, granite gneiss, augen gneiss and pegmatite;
Xcc Caicara Formation	Early Proterozoic	Rhyodacite to rhyolitic tuffs, porphyries, flows, dykes and granophyre.
Xg	Early Proterozoic	Calc-alkaline granites
Xgu	Early Proterozoic	Undivided intrusive rocks
Xmo	Early Proterozoic	Moriche, Cinaruco and Esmeralda Formations
Xyr	Early to Middle Proterozoic	Roraima Group and Pre-Roraima undivided sedimentary rocks
MP-Mmbg1 Roraima-La Pedrera Formations	Mesoproterozoic	Metaconglomerates, metasandstones, quartzites, and metapelites with low grade regional metamorphism
Ylg	Middle Proterozoic	Silicic intrusive rocks
Ypg/MP-Pf1 Parguaza Granite	Middle Proterozoic	Rapakivi granite
N1-Sc	Miocene	Conglomerates and sandstones. Poorly consolidated
Qal/Q-e/Q-t/Q-al	Quaternary	Alluvial, eolic and terrace deposits

zones within cratonic areas, where a characteristic geochronological pattern predominates, and the age determinations obtained by different isotopic methodologies for different geological units are coherent (Tassinari and Macambira, 1999). Geological provinces are a region or area of large extent with similar features throughout and capable of being considered as a unit (Allaby, 2013). For the Amazonian Craton, geological provinces are areas with its own geological, structural, magmatic and isotopic features (Santos et al., 2000). The VTP/RNJ and Rionegro provinces represent areas of juvenile continental crust, accreted by stacking of successive magmatic arcs, probably produced by subduction of oceanic lithosphere at the beginning of the collision between the older provinces of the Amazonian craton and another continental mass which is now probably part of the younger provinces and Laurentia (Tassinari and Macambira, 1999; Santos et al., 2000; Cordani et al., 2016b; Kroonemberg, 2019). Cordani et al., 2016b also concluded that the possible NE boundary of the RNJ province with the older VTP would be located close to or along the international boundary between Colombia and Venezuela.

Geophysical interpretation of the principal tectonic domains in Brazil (Gusmao and Freitas, 2014) finds that the proposed extend of the VTP is characterized by a positive NW-SE Bouguer anomaly. Also, they concluded that its limits with the other provinces are well defined by gravity gradients that may register the superposition of crustal fragments with different density.

2.2. Structural and tectonic framework

Structural and tectonic features within the basement rocks (Gómez et al., 2019; Gómez et al., 2015b) are scarce in Colombia due to the sedimentary coverage compared to the east (Fig. 4a), where more structural data are available (Hackley et al., 2005).

Graterol (2009) interpreted structural features from airborne gravity and magnetometry data on the north and east Llanos Basin in Colombia. This interpretation suggests the presence of structural highs and lows on

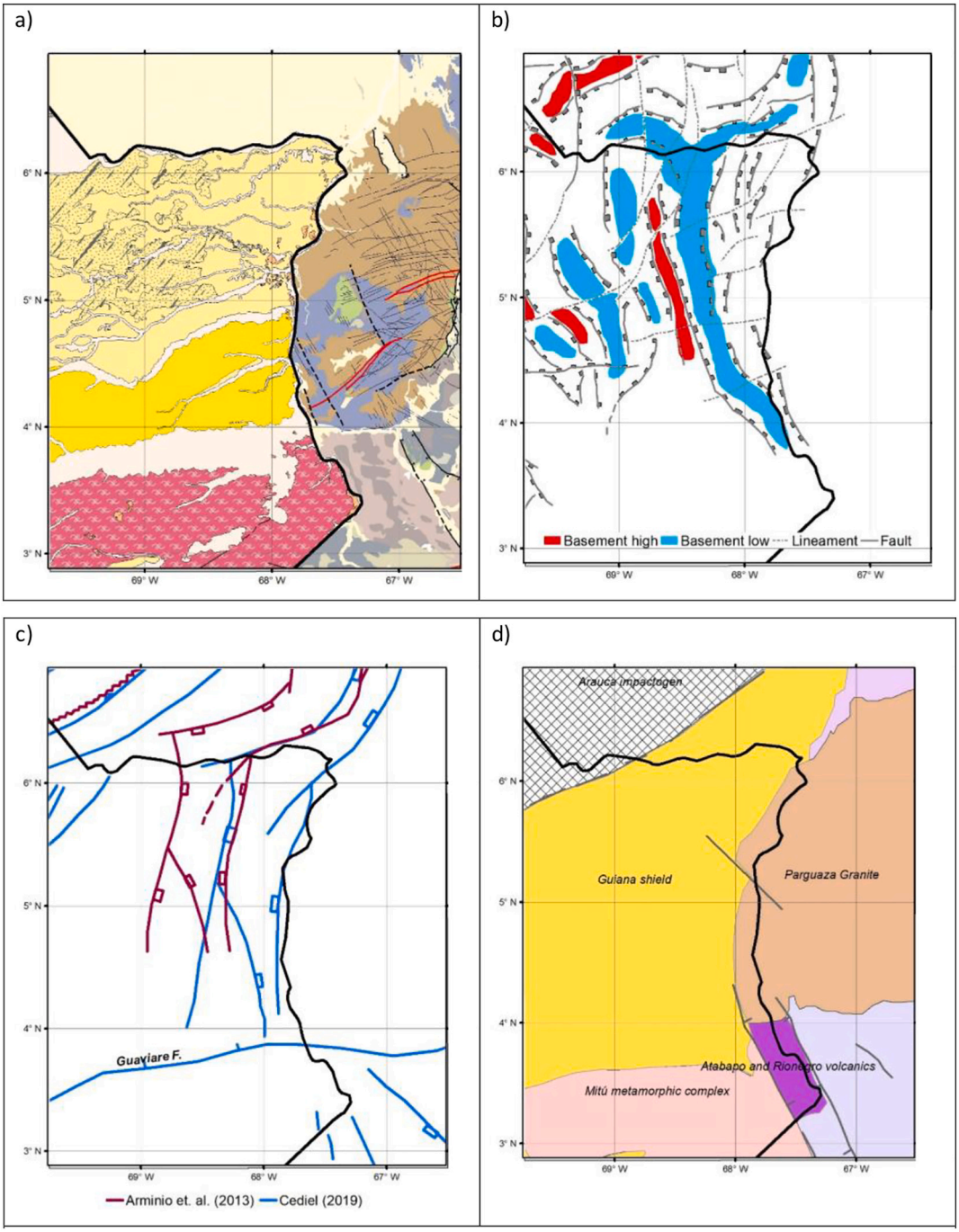

Fig. 4. a) Regional geology (Fig. 3). b) Structural interpretation to the top of the Paleozoic. (Modified from Graterol, 2009). c) Location of the Mantecal Graben (red lines, modified from Arminio et al., 2013) and structural sketch map. (blue lines, modified from Cediel, 2019). d) Paleogeography sketch map with relevant Meso and Neoproterozoic tectonostratigraphic units (Modified from Cediel, 2019). (For interpretation of the references to colour in this figure legend, the reader is referred to the web version of this article.)

the Precambrian basement, controlled by NNW-SSE normal faults that created possible sedimentary basins (Fig. 4b). Arminio et al. (2013) proposed the existence of the "Mantecal Graben" (red lines, Fig. 4c), a NNE-SSW structure extended from Venezuela to the south into Colombia, supported by the presence of folded Neo-Proterozoic(?) sandstones of the Cinaruco Formation exposed on the eastern shoulder of the Graben.

Recent work of Cediel (2019) combined interpretation from multiple sources to integrate a paleogeographic sketch map with relevant Meso and Neoproterozoic tectonostratigraphic units for the Guyana Shield (Fig. 4d). This sketch marks an important structure to the NW of the area as the "Arauca Impactogen" (San Fernando Graben in González et al., 2017) and the Atabapo and Rionegro rifts to the SE. This work also presented a structural sketch map of south America (blue lines, Fig. 4c) that, for the study area, delineate the E-W Guaviare Fault at the south and NNE-SSW normal faults that control the Mantecal Graben, and NNW-SSE faults that control the Rionegro and Atabapo Rifts.

Fig. 4 reflects the present-day knowledge of the geology and tectonic evolution of the Amazonian Craton for the Colombian portion of the study area, that is supported by regional-scale geophysical data interpretation and comparison with geological information from nearby areas. A significant range of models have been proposed for the same

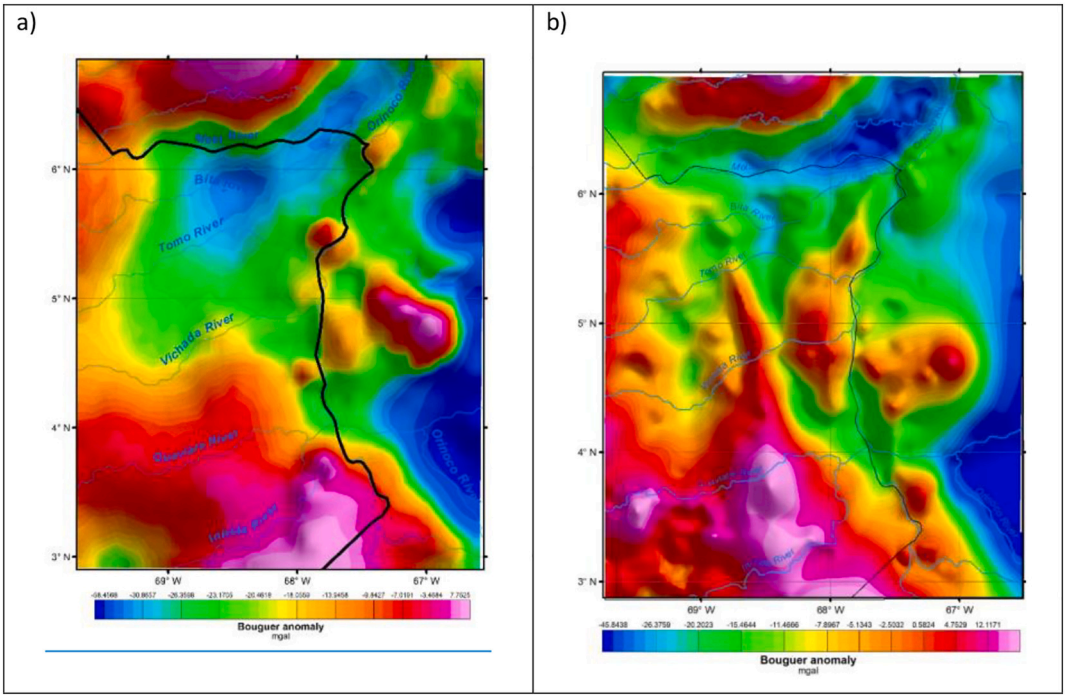

Fig. 5. Gravity dataset used. a) Bouguer anomaly EIGEN 6C4; b) Bouguer anomaly ANH.

geological region (see Fig. 4), highlighting our still misunderstood Amazonian Craton in the region.

3. Geophysical datasets and processing

Major deformation events, crustal-scale accretions and magmatic activity episodes could potentially produce identifiable crustal heterogeneities characterized by spatial variations in physical properties of the rocks. Gravity and magnetic methods measure lateral variations of the Earth's gravity and magnetic fields, sensitive to density and magnetic susceptibility variations of the rocks within the crust. Previous studies demonstrate how potential fields can help understand the geological setting of the Amazon Craton and other areas with similar structural and tectonic complexity (Gusmao and Freitas, 2014; Baines et al., 2009; Baines et al., 2010; De Castro et al., 2013; Gusmao et al., 2005; Heath et al., 2009; Isles and Rankin, 2013; Yan et al., 2011).

A technique to process potential field data to study structures and tectonic boundaries is the multiscale edge detection or "worming" (Horowitz et al., 2000; Heath et al., 2009; Crawford et al., 2010; Yan et al., 2011; FitzGerald and Milligan, 2013; Kohanpour et al., 2018). The main purpose of this technique is to locate the edges of magnetic and gravity sources from gravity and magnetic field anomaly maps (Blakely and Simpson, 1986). The process includes the location of points of maximum value on a map of horizontal gradient magnitudes. These points can be joined into lines to form a 2D "pseudo-geology" image (Heath et al., 2009). The application of these steps at multiple upward continuation levels of the potential field data constraints the position and strength of the edges of the sources, and the results can be interpreted in terms of the 3D architecture and depth extend of geological structures (Yan et al., 2011). This technique could represent a compromise between a mostly qualitative "visual inspection" and a mostly quantitative determination of the vertical and horizontal extent of geological bodies (Hornby et al., 1999; Baines et al., 2009; Bird, 2001; Ferreira et al., 2011; Park et al., 2013; Soares and Da Costa, 2013; González et al., 2017; Geng et al., 2019).

3.1. Previous geophysical studies

Graterol (2009) calculated the depth to the top to the Paleozoic and Precambrian basement using an inversion algorithm based on the gravitational attraction of vertical prisms. Moyano et al. (2018) presented modelling and interpretation of regional to local magnetic anomalies using a 3D inversion of the magnetization vector (MVI, Ellis et al., 2012). The surface projection of the magnetic sources modelled were presented as polygons with information about the depth to the causative magnetic body and magnetic susceptibility cutoff from the 3D model.

Other studies focused on qualitative interpretation of potential field maps to provide geological information about the structure of the Amazonian Craton in the area. Kroonenberg and Reeves (2012) analyzed available gravity and magnetic maps of the Amazonian Craton in Colombia to delineate some major structures and basement features. De Boorder (2019) presented a revised version of a structure in eastern Colombia named "La Trampa Wedge" (De Boorder, 1981) supported by magnetic images presented by Kroonenberg and Reeves (2012). In Celada et al. (2006, see appendix) the delineation of magnetic domains and other linear features south of the area of interest are presented, without additional geological/tectonic interpretation.

3.2. Geophysical datasets

Available gravity and magnetic datasets vary from low-resolution/world coverage gravity (EIGEN 6C4, Förste et al., 2014) and magnetic anomalies (EMAG2V3, Meyer et al., 2017) to detailed/regional coverage compilations from the Colombian Hydrocarbon Agency (ANH) and the Servicio Geológico Colombiano (SGC) (Graterol and Vargas, 2010; Moyano et al., 2018).

In this study we use gravity (Fig. 5) and magnetic (Fig. 6) datasets from EIGEN6C4, EMAG2V3 and the ANH that provide a comprehensive coverage of the region of interest, and include the high-resolution airborne magnetic anomaly map from the SGC (see Table 2 for a more complete technical specification of all datasets). We also provide Supplementary Figs. (S1 and S2) with the location of the observation points for ANH gravity (ground and airborne) and magnetic (airborne)

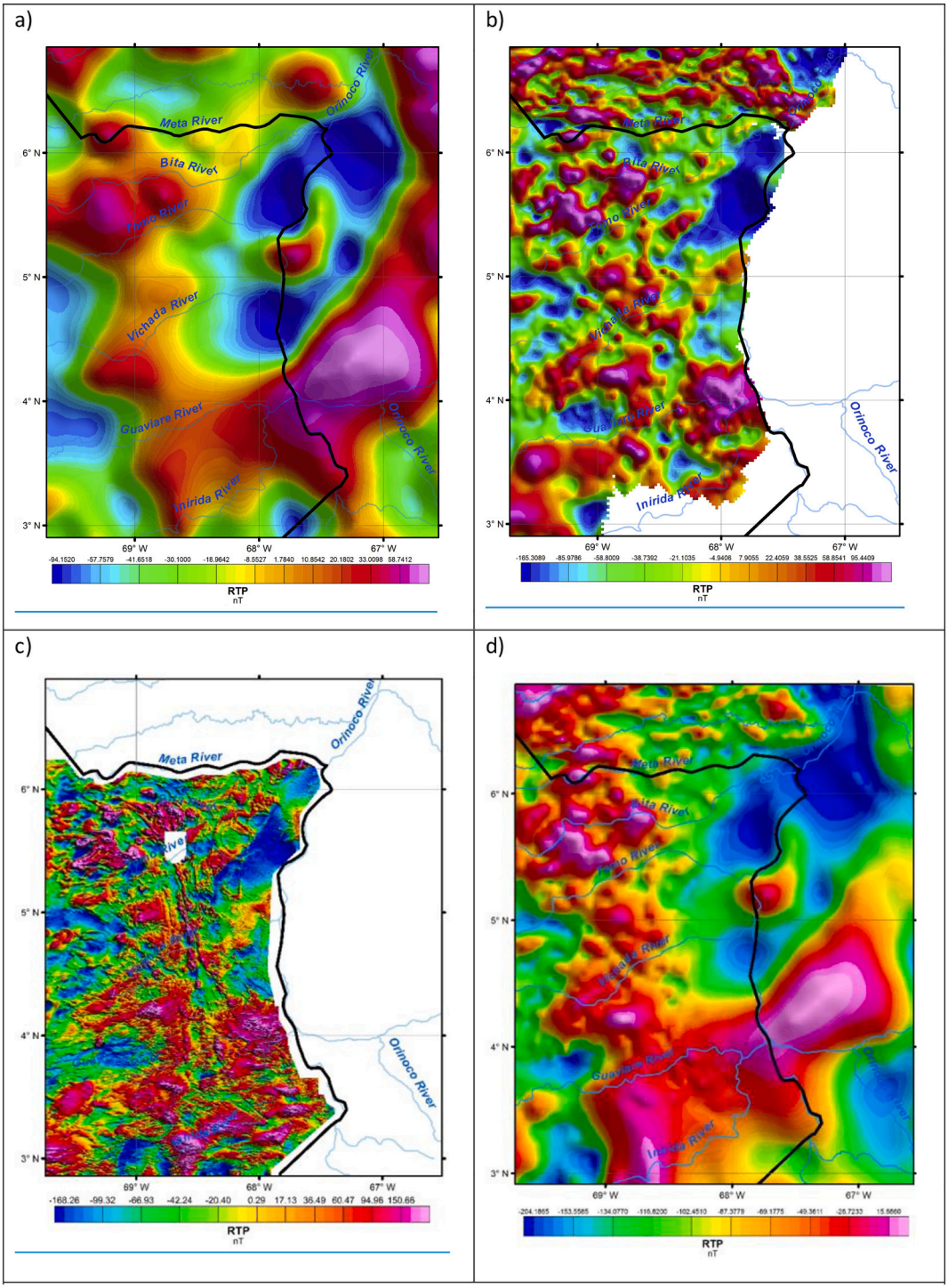

Fig. 6. Magnetic dataset used: a) Reduction to magnetic pole EMAG2V3; b) Reduction to magnetic pole ANH; c) Reduction to magnetic pole SGC; d) Reduction to magnetic pole of merged EMAG2V3 and ANH.

datasets, respectively.

To construct a single magnetic grid of regional coverage, dataset from ANH were upward continued to 4.000 m and merged with EMAG 2 V3 grid, using "Gridknit" extension provided with Oasis Montaj software (Geosoft). Merged-regional magnetic grid is presented in *Fig. 6*d.

3.3. Data processing and interpretation

As was pointed out above, geological and structural models of the Amazonian craton in the study area are mostly qualitative, based on geophysical data. This explains why the tectonic framework of the craton itself remains under debate (Graterol, 2009; Arminio et al., 2013; Cediel, 2019; De Boorder, 2019; Kroonemberg, 2019). We integrate previous geological observations and well-known geophysical processing techniques (Horowitz et al., 2000) to provide new information about the structural configuration of the basement rocks and upper crust in the study area.

3.3.1. Magnetic domains and lineaments

Qualitative interpretation of linear features and magnetic domains

Table 2
Technical specifications of the geophysical datasets used.

Source	Type	Dataset spec.	Coverage of study area
EMAG2V3	Satellite, ship, airborne magnetics.	Data points each 4.000 m., leveled at 4.000 m altitude. Gridded at 5 × 5 km cell size	Complete
EIGEN6C4	Satellite, surface Gravity	Data points each 10.000 m. Bouguer density: 2.67 g/cm^3 Gridded at 10 × 10 km cell size.	Complete
ANH	Airborne/surface gravity & Airborne magnetics.	Variable between projects, Grid with 2.500 m point separation and leveled at 1.200 m altitude. Bouguer density: 2.67 g/cm^3 Gridded at 2.5 × 2.5 km cell size	Gravity: Complete Magnetometry: Partial
SGC	Airborne Magnetics /Gamma. Single project with multiple blocks flew from 2013 to 2017.	Distance between flight lines: 500 m to 1000 m. 100 m altitude above terrain. Gridded at 250 × 250 m cell size	Partial

were performed using the reduced to pole (RTP, Baranov, 1964) dataset of *Fig. 6*c. This magnetic dataset has a resolution that allows to recognize linear features in the magnetic basement and to delineate different magnetic domains. The dataset was processed to calculate the total horizontal gradient from the RTP (Fig. 7a). The total horizontal gradient represents the maximum gradient in the vicinity of the observation point (Dentith and Mudge, 2014). Regions with sharp variation and irregular features (strong gradients) are highlighted in the image; for example, spatially coherent discontinuities will have high intensity allowing for the visual recognition of objects and patterns of the image (Hornby et al., 1999).

The qualitative interpretation of magnetic data indicates that there are lateral variations in the structural framework and magnetic properties of the basement rocks across the area. These lateral variations can be grouped roughly into four "zones" (Fig. 7b). The southern (red) area shows predominantly NW-SE and NE*E*-SWW features; the central (yellow) area has predominant NEE-SWW lineaments. These two areas are separated by a NEE-SWW lineament that cross all the study area, that clearly cuts the continuity of the NW-SE lineaments of the red area and that is located to the south of the Guaviare Fault (Fig. 4c). The northern (green) area is separated from the central (yellow) area by the transition from mostly NEE-SWW lineaments to NE-SW/NW-SE linear features to the north. The central parts of the middle and northern areas are crossed by a narrow strip (blue region) with predominant N-S lineaments.

Linear features interpreted from magnetic data (Fig. 7b) shows significant variations across the area. In the red area, NEE-SWW linear features predominate over NW-SE lineaments. Along the yellow area, almost all linear features have E-W to NEE-SWW trends and on the green area lineaments are equally NW-SE and NE-SW. Non-linear features are predominant at the east of the green area principally.

Areas with abrupt lateral changes in the frequency and/or amplitude of the horizontal gradient were interpreted as possible changes in the distribution of the magnetization of the basement rocks (Blakely and Simpson, 1986). These areas were delineated in different magnetic domains (Fig. 8), that are in many cases limited by sharp edges with strong gradients. For example, the magnetic domains F, G, K in Fig. 8, have a circular shape and can be easily observed in Fig. 7a.

We want to highlight a remarkable domain with high gradients ("C", Fig. 8) that strikes N-S and extends from about 3.5 N to 5.5 N, and corresponds to the Blue Area in Fig. 7b. This region seems to correlate with the basement high interpreted by Graterol (2009) (Fig. 4b). Also, this N-S domain cuts many of the magnetic lineaments of the central and northern zones (yellow, green, Fig. 7b) and apparently separates two medium to low-gradient areas (lighter colors, Fig. 7a) marked as domains A and B in Fig. 8.

3.3.2. *Multiscale edge detection "worming"*

Multiscale edge detection applied to the potential field data of the study area follow the steps described by Heath et al. (2009). First, the

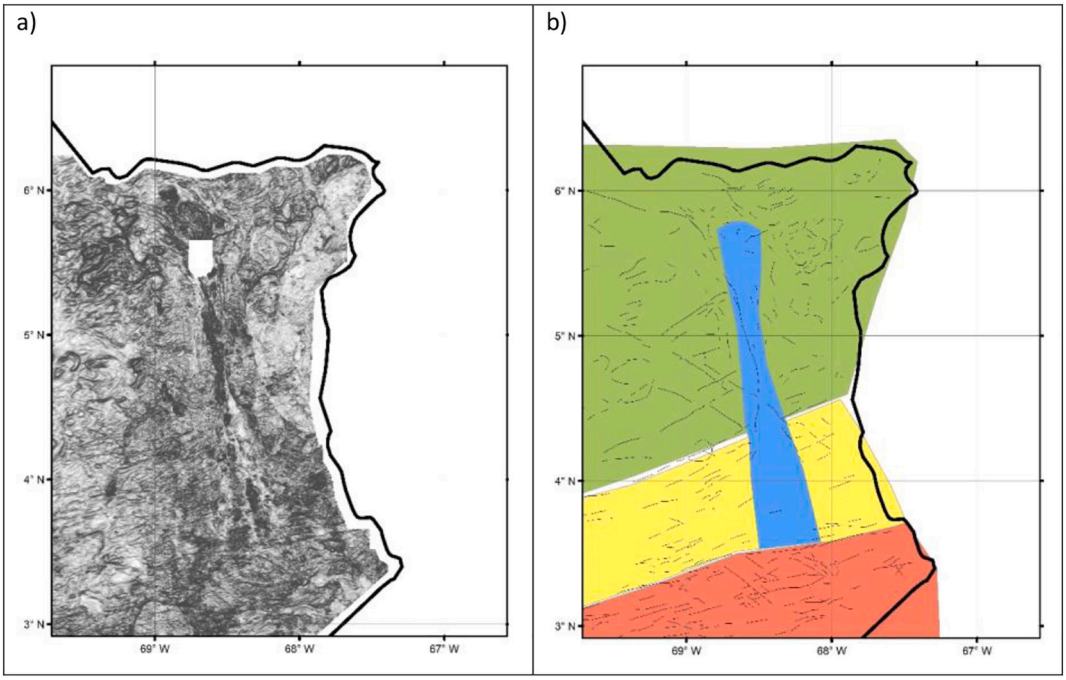

Fig. 7. a) Horizontal gradient of the RTP (dataset: Geological Survey of Colombia); b) Structural zones interpreted from magnetic data.

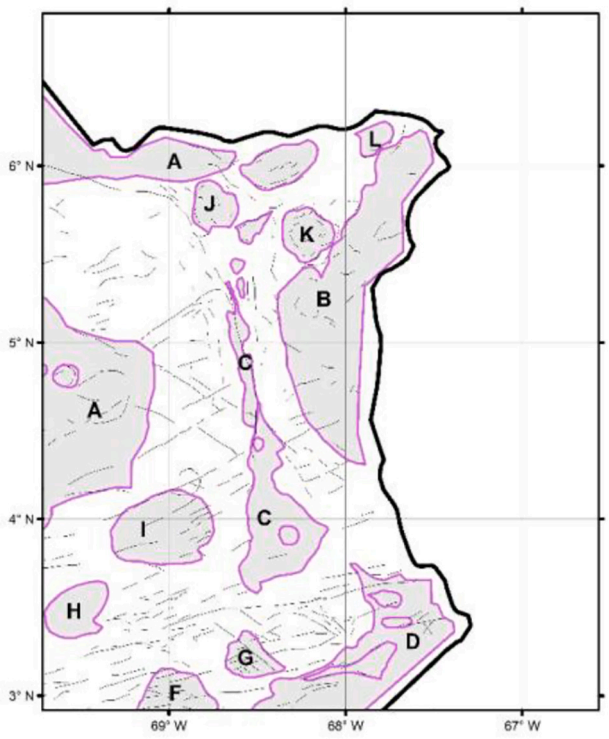

Fig. 8. Interpretation of magnetic lineaments and domains.

potential field maps (Bouguer anomaly and Reduction to magnetic pole) were upward continued to various levels. Second, the horizontal gradient for each level were computed and the points of maximum slope were delineated. For the location of maxima points in the horizontal gradient grid were applied the method presented by Blakely and Simpson (1986) that is included in the "Source Edge Detect" extension of Oasis Montaj (Geosoft).

The process described above were applied to the Bouguer anomaly grid (Fig. 5b) and the magnetic data of Fig. 6a and Fig. 6b. Upward continuation levels applied were 2, 4, 8, 16 and 32 km for gravity data and 0.5, 1, 2, 3, 4, 6, 8, 16 and 32 km for magnetic data. The integrated maps are presented in Fig. 9. It must be pointed that the upward continuation distance does not mean a specific depth (Heath et al., 2009).

The worms interpreted from gravity data (Fig. 9a) delineate some structures that, by its coherency on the multiple levels of upward continuation, can be interpreted as features that affect the basement and may also have deep penetration into the upper crust. Some of these features can be correlated with geological contacts in the Amazonian Craton in Venezuela. An example is at the SE of the area (red box, Fig. 9a) were the multiscale edges delineate the contact of the Parguaza Granite with rocks of the Cuchivero Group and a N*E*-SW normal fault reported by (Hackley et al., 2005) (Fig. 9d) and that corresponds roughly to the eastern limit of the "Rionegro and Atabapo volcanics" tectonostratigraphic unit of Cediel (2019) (Fig. 4d).

In Colombia, the most remarkable features are three parallel worms with NNW-SSE orientation (Fig. 9a). The central edge extends more than 200 km northward and then bends to the W. The configuration of the edge at multiple scale visualization (Holden et al., 2000) indicate that it can be a nearly vertical feature with a subtle inclination to the east from 5 N to the north. The edge located to the west extends between 4.2 N and 5.2 N and have a subtle inclination to the west. The edge located to the east extends NNW-SSE between 4.2 N and 5.3 N and then bends to the NE. This last edge has a subtle inclination to the east on its NNW-SSE portion. These NNW-SSE worms correlate with some of the normal faults interpreted by Graterol (2009) (Fig. 4b) but clearly are in a different structural direction and position from the NNE-SSW Mantecal graben (Fig. 4c) reported by Arminio et al. (2013) and Cediel (2019).

Another feature of interest is a series of short, vertical, *E*-W edges located along 4 N and that apparently limit the extension to the south of the NNW-SSE edges described above. This nearly E-W edge correlates with the Guaviare Fault reported by Cediel (2019) (Fig. 4c).

Worms from magnetic data (Fig. 9b) are more random at the "shallow" levels of upward continuation that can be associated to shallow sources and noise. However, the medium to "deep" boundaries show similar correlations with the gravity edges and geological structures, like the SE limit of the Parguaza granite in Venezuela. In Colombia, some coherency between the gravity and magnetic features is found, like the central and northern portion of the western NNW-SSE feature that extends from 4.2 N to the north-northeast (blue box, Fig. 9b). Also, it must be noted that the E-W feature along 4 N (Guaviare Fault) is more evident in the magnetic data.

Fig. 9c shows the principal boundaries identified from the joint interpretation of the gravity and magnetic worms, and the integration of these boundaries with the qualitative interpretation of magnetic data and available structural information are shown in Fig. 10.

From Fig. 10 we emphasize that the deep, crustal penetrating features identified by "worming" are closely related to the structural framework and boundaries of the domains described in the qualitative interpretation. This correlation indicates that the linear features and lateral variations on the magnetization of the basement rocks, associated with deep penetrating edges interpreted from gravity and magnetic data, could also reflect boundaries between different tectonic domains.

3.3.3. 3D inversion of gravity and magnetic data

3D inversion of selected gravity and magnetic datasets allows to estimate the regional distribution of the physical properties (density and magnetic susceptibility) in the basement rocks. Density and magnetic susceptibility models can provide valuable information to explain the variations in the measured gravity and magnetic fields and hence to integrate a more robust framework to the qualitative and multiscale edge detection interpretation.

For the 3D modelling of the geophysical data were used VOXI Earth Modelling (Geosoft). A starting model of 2500x2500x500 meters cell dimension were built for density and magnetic susceptibility (MVI) inversion. To remove high frequency anomalies related to shallow sources, gravity data of Fig. 5a were upward continued to 4.000 m and a low pass-filter of 15 km wavelength was applied to the magnetic data of Fig. 5e. Magnetic susceptibility inversion used the Magnetization Vector Inversion algorithm (MVI) that incorporates both remanent and induced magnetization. MVI inverts jointly the intensity and direction of magnetization, allowing the magnetization vector to vary direction throughout the inversion area (MacLeod and Ellis, 2013). This approach has better results understanding that non-induced magnetization plays a far more important role than previously thought in the origin of magnetic anomalies (Ellis et al., 2012).

The density distribution calculated by inversion of gravity data (Fig. 11a) range from 2.52 g/cm^3 (blue) to 2.9 g/cm^3 (red/cyan). Magnetic susceptibility estimated by the amplitude of the magnetization vector (Fig. 11b) range from 3.7×10^{-6} SI (blue) to 0.05 SI (cyan).

Due to the limited geological information that can be used to constrain the models for a great portion of the study area, interpretation should be addressed carefully due to the non-uniqueness principle of the inversion of geophysical data. However, both density and magnetic susceptibility models computed for the study area shows good correlation with the possible geotectonic domains identified by qualitative interpretation and multiscale edge detection.

Fig. 12a shows the plan view of the zones with density higher than 2,71 g/cm^3 (magenta) and lower than 2,69 g/cm^3 (blue). These sources are located principally at 4 to 4.3 km below the surface and shows correlation with the edges of the domains interpreted, like the central NW-SE and eastern domains. Zones with magnetic susceptibility higher

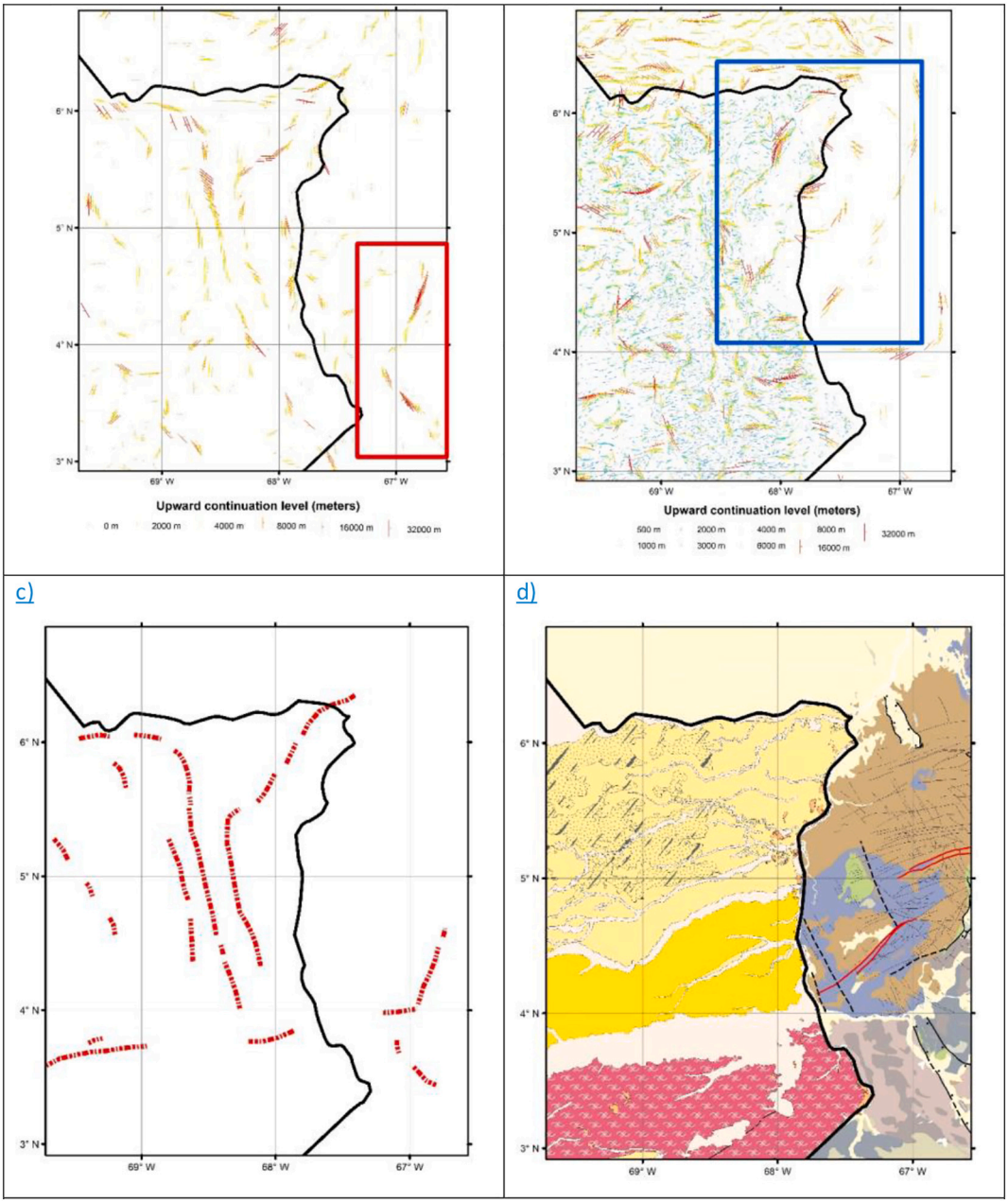

Fig. 9. "Worming" results on the study area. a) from gravity data; red box: worms correlated with tectonic boundaries (see text). b) from magnetic data; blue box: example area with correspondence between gravity and magnetic worms. c) principal edges interpreted from gravity and magnetic worms; d) Regional geology from Fig. 3. (For interpretation of the references to colour in this figure legend, the reader is referred to the web version of this article.)

than 0.01 SI (Fig. 12b) also show some correlation with regional features: magnetic sources are shallower at the NW of the area (<1 km) and deeper to the SW (~2 km) and east (>7 km). It is evident that almost all the magnetic sources are located north of the *E*-W boundary recognized in the multiscale edge detection, and that the deepest sources at the east are limited by the easternmost NNW-SSE boundary interpreted.

4. Discussion

As pointed above, the NW portion of the Amazonian Craton is one of the least geologically known areas in the world. To overcome that restrictions, geophysical datasets that register the lateral variations in the earth's gravity and magnetic fields over the study area were used. Geophysical data were processed and interpreted to associate the field responses with density and magnetic susceptibility variations in the upper crust.

The most widely accepted models for the evolution Amazonian Craton (Fig. 2) propose that the Craton evolved from an ancient nucleus by successive accretion of younger terrains/provinces. The Ventuari-Tapajos (VTP) and Rionegro-Juruena (RNJ) geochronological provinces (Tassinari and Macambira, 1999) or the Rionegro geological province (RNP, Santos et al., 2000), represent juvenile continental crust accreted to the older provinces by stacking of successive magmatic arcs. Cordani et al., 2016b proposes two NW-SE belts in the Mitú Complex (Atabapo and Vaupés belts) formed by stacking of magmatic arcs in different pulses of orogenic activity. Of these belts, the Atabapo belt should be located at the SE of the study area, nearly parallel to the border between Colombia and Venezuela.

Available structural interpretations and sketches for the study area (Fig. 4) used principally geophysical data to identify lineaments and

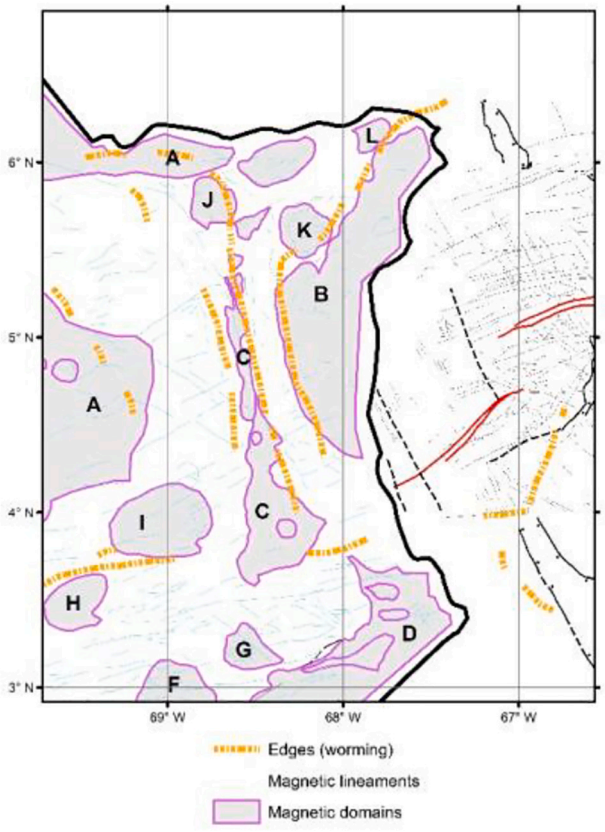

Fig. 10. Interpreted boundaries by "worming" of potential field data with magnetic lineaments/domains and structural data of Hackley et al. (1995).

faults in the Precambrian basement and to delineate basement high and lows that define sedimentary basins. However, these models did not explain the tectonic complexity and rock variability of the crystalline basement that is evident in the areas where it is exposed. To explore this complexity, various geophysical datasets were used (Fig. 5) to provide an interpretation of the structural and tectonic framework of the Amazonian Craton in the study area. The processing techniques applied to the geophysical data were qualitative/semi-qualitative interpretation and quantitative modelling of the distribution of the physical properties of the upper crust.

Lineaments and magnetic domains in Colombia area were interpreted from the total horizontal gradient of the RTP image of the higher resolution airborne magnetic data acquired by the SGC (Fig. 7a). This transformation of the geophysical data allowed to enhance the sharp lateral variations of the magnetized rocks below the almost non-magnetic sedimentary coverage. For Venezuela area geologic structures from the map of (Hackley et al., 2005) were used.

Qualitative interpretation of the main magnetic lineaments (Fig. 7b) shows that the study area can be divided from south to north into three zones (Southern, Central and northern; red, yellow and green respectively). The central and northern zones are also crossed by a fourth, narrow zone (blue) with predominant N-S lineaments. The predominant NE*E*-SWW structural pattern in the central zone is different than the northern and southern zones. Also, this central zone truncates most of the magnetic lineaments of both north (green) and south (red) zones, so we propose that the central zone reflects a later deformation event. From this point of view, this central zone could represent a regional NEE-SWW shear zone that extend from west of the study area to the east into Venezuela, where some nearly E-W transverse faults are mapped (Fig. 17). In Colombia, 1:100.000 scale geological maps register NEE-SWW left-lateral faults with normal component located in the yellow zone (Rio Guaviare and Mataven faults) and at the SE part of the green zone (Rio Vichada and Rio Tuparro faults).

Magnetic domains (Fig. 8 and Fig. 10) can be interpreted as areas with similar magnetic minerals content and distribution or, in a simple approximation, to the same lithology. The domain B (Fig. 8) is characterized by a regional magnetic low (Fig. 6) and is partially coincident with the exposure of the Parguaza granite in Venezuela. This domain is interpreted as the magnetic expression of rocks related with this geological unit (Fig. 17). It should be noted that recent geological maps (Alfonso et al., 2014) report exposures of the Parguaza Granite to the west of this magnetic domain (blue dot, Fig. 3).

At the south of the area, a polygonal domain (F) has similar gradient texture of the above mentioned. Also, it shows straight NW-SE and NEE-SWW lineaments that contrast with the surrounding area. This domain delimitate an intrusive body identified as the "Matraca Rapakivi Granite" (Bonilla et al., 2016; Bonilla, 2019). This correlation allows to expect that some of the other rounded to polygonal domains (G, H, I, J, K, L) can also constitute intrusive bodies (Fig. 17).

Possible boundaries identified by the multiscale edge detection technique are coherent with the structural/tectonic domains delineated by the qualitative interpretation (Fig. 10). The easternmost NNW-SSE edge are coherent with the magnetic domain (B) that are associated with the Parguaza Granite. This edge could be interpreted as the expression of the intrusive contact of the Parguaza Granite with the basement rocks of the Craton. The edge located at the SE of the area, that also delineate the contact of the Parguaza Granite with the Cuchivero Group, illustrate the deep expression of this intrusive contact (red box, Fig. 9a).

The central and western NNW-SSE edges are associated with the boundaries of a high density/high magnetization domain that extends from 3.5 N to the North and have predominantly N-S orientation (Fig. 5, Fig. 10 and Fig. 12). This area corresponds to the structural zone (blue zone, Fig. 7b) that truncates the NW-SE and N*E*-SW lineaments present at the east and west of the area. It is important to mention that the NNW-SSE edges are coincident with important changes in the course of the Bita River (Fig. 13) that suggest tectonic control on the drainage that is also slightly present in the Tomo and Vichada rivers.

This NNW-SSE zone represents an important feature that clearly cuts the structural continuity of the central and northern zones. This feature was recognized by Graterol (2009) as a high density/high magnetic susceptibility source that forms a NNW-SSE basement high delimited by normal faults (Fig. 4b). Also, Arminio et al. (2013) and Cediel (2019) proposed a NN*E*-SSW graben structure (Mantecal Graben, Fig. 4c) for the same area. Our interpretation and geophysical 3D modelling support the presence of dense, magnetic source(s) within this area, as was proposed by Graterol (2009). However, the new datasets and interpretations presented in this work allow us to speculate that this narrow NNW-SSE zone could represent a deep-penetrating/crustal scale discontinuity, like an aborted rift with intrusion of dense, magnetic mafic bodies or a suture zone with accretion of a volcanic arc (Fig. 17). More work should be done in this area to investigate the geological processes involved.

.

The NNW-SSE edges mentioned above are limited to the south by an NEE-SWW edge, located at the center of the zone with predominant NEE-SWW lineaments (yellow zone, Fig. 7b). This edge controls the course of the Guaviare River in Colombia and the Orinoco and Ventuari rivers in Venezuela (Fig. 13). This structure was reported by Cediel (2019) as a normal fault (Guaviare Fault, Fig. 4b). However, with the new data obtained in the present work, it is clear that this feature corresponds to a deeper crustal discontinuity that may produce the strong E-W orientation of the magnetic lineaments and can be related to some transcurrent faults mapped in Colombia and Venezuela.

Density model for the study area (Fig. 12a) show that the edges interpreted are also characterized by strong contrasts between high and low density bodies. This can be related with the interpretation of Gusmao and Freitas (2014) that strong gravity gradients register the superposition of crustal fragments with different densities and probably

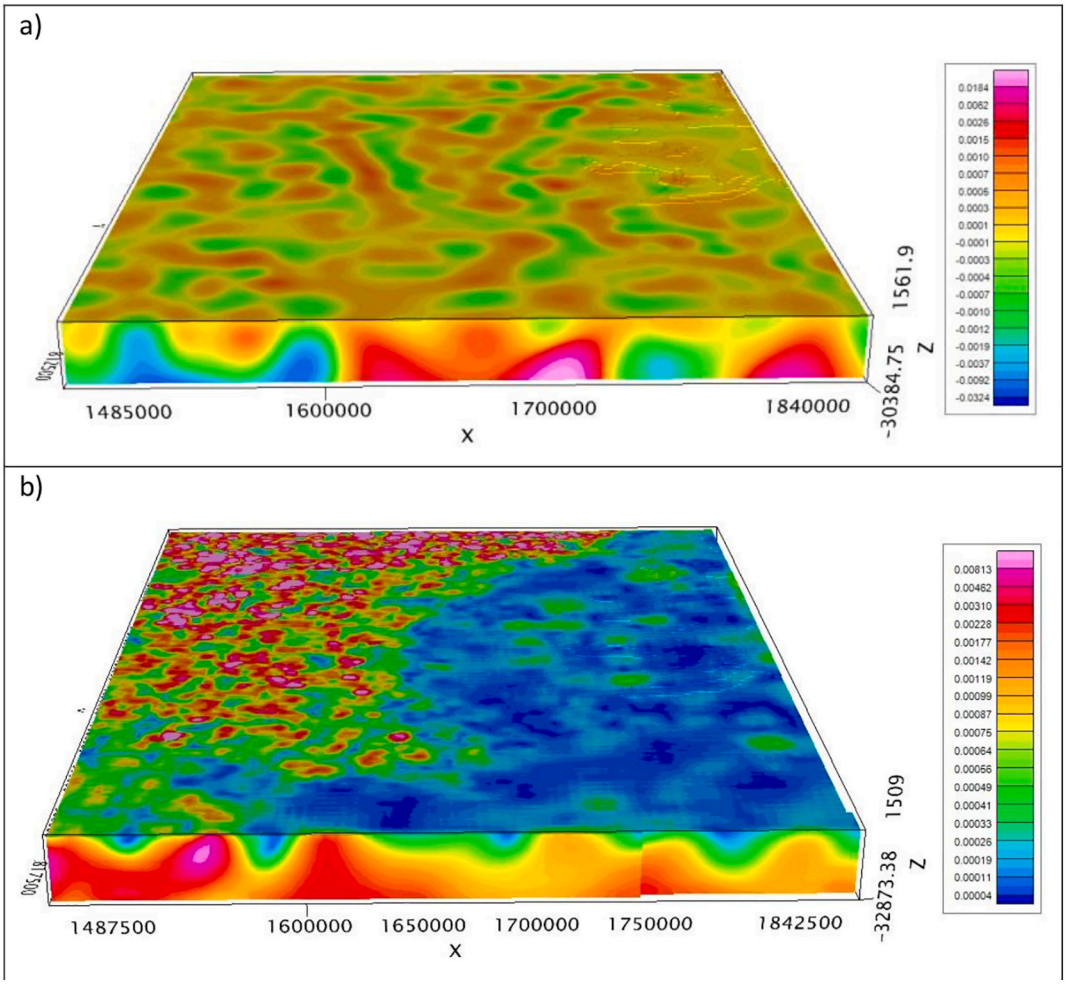

Fig. 11. (a) Density model. Colorbar: Density variation from reference 2,67 g/cm^3; (b) Magnetic susceptibility model (Amplitude of the magnetization vector). Colorbar: Magnetic susceptibility (SI).

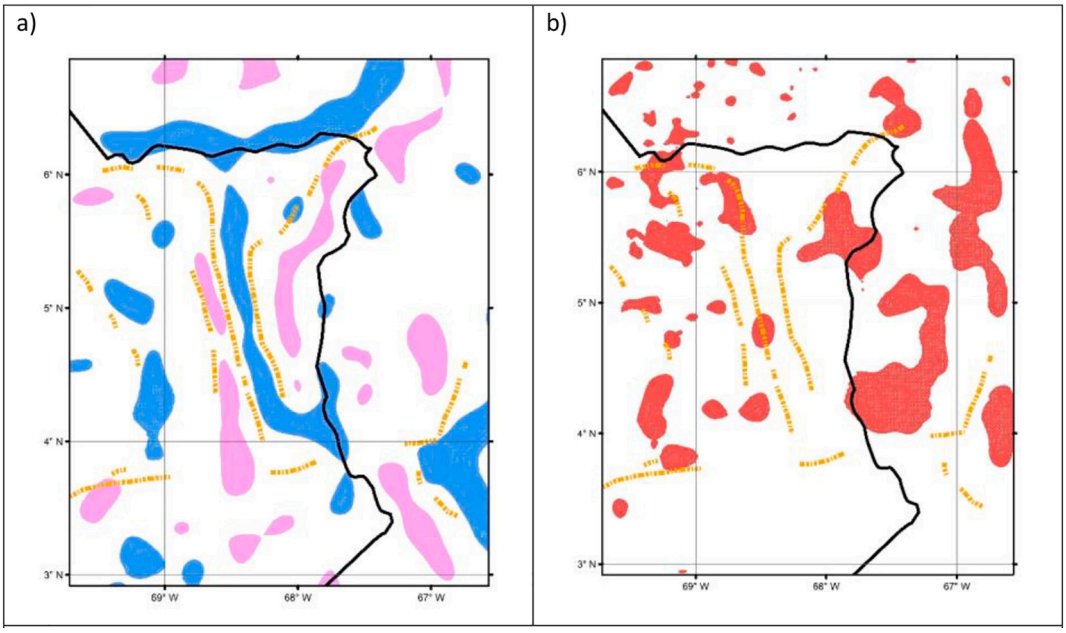

Fig. 12. a) plan view of isosurfaces around densities higher than 2,71 g/cm^3(Magenta) and lower than 2,69 g/cm^3 (blue); b) plan view of isosurfaces (red) around magnetic susceptibilities higher than 0.01 SI. (For interpretation of the references to colour in this figure legend, the reader is referred to the web version of this article.)

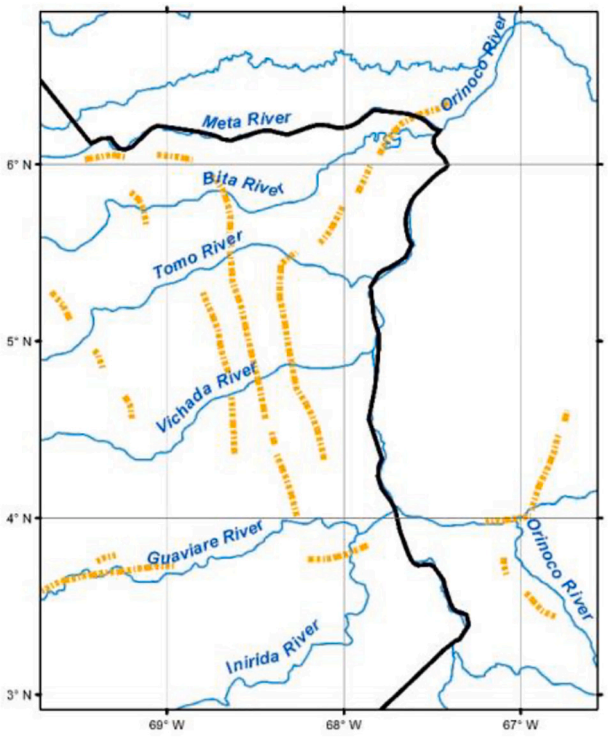

Fig. 13. Boundaries interpreted and principal drainages of the area.

reflects the stacking of magmatic arcs during the formation of the VTP and RNJP. Also, density and magnetic susceptibility models of the Gawler Craton (Australia, Baines et al., 2009) shows that major changes in the physical properties correspond with major changes in lithology associated to the edges of major tectonic events. High magnetic sources (Fig. 12b) are more scattered, but its distribution and depth zonation are still coherent with the edges interpreted.

Cross sections of the density (Fig. 14b) and magnetic susceptibility models (Fig. 14c) along a W-E profile show the high variation in the density and magnetic susceptibility across the central and western NNW-SSE edges (red square) but the eastern border, associated with the Parguaza Granite, only shows high density contrast. Similarly, the NNE-SSW edge that follow the contact of the Parguaza Granite with the Cuchivero Group at the SE of the area (black square) have strong density contrast but no magnetic susceptibility expression.

The NW-SE edge located at the SE of the area parallel to the left margin of the Orinoco River is another relevant feature by its high-density contrast and correlation with the study of Cordani et al., 2016b, that concluded that the boundary between Rionegro-Juruena and Ventuari-Tapajós provinces will be located close to or along the Atabapo River. Also, Gusmao and Freitas (2014) reported high-gravity gradient features near the border of the Ventuari-Tapajós province in Brazil. The interpretation of our study locate the possible boundary of the VTP with RNJ Provinces (Tassinari and Macambira, 1999) eastward from the actual location (Fig. 2a and Fig. 17).

Depth slices from density (Fig. 15) and magnetic susceptibility models (Fig. 16) at 5 km, 10 km and 15 km also show the coherence and deep penetrating character of the edges interpreted. These edges are clearly related to major crustal features that also may correspond to tectonic boundaries.

The direction movement of the nearly E-W edge located at 4 N cannot be clearly established: while geological maps shows dextral/normal faults that apparently control some of the drainages of the area, it must be noted that the gravity and magnetic datasets (Fig. 5 and Fig. 6) and the interpretation maps and models of the present work show apparent right-lateral displacement of the deep penetrating anomalies along this boundary. Nevertheless, the emplacement of the Parguaza Granite also can be responsible of this tectonic control on the geophysical anomalies.

5. Conclusion

The present work focused on qualitative and quantitative interpretation of gravity and magnetic data in NE Colombia. The results suggest a complex structural and tectonic framework on the Amazonian Craton that was not registered in the available maps and models.

Magnetic lineaments from the total horizontal gradient of the reduction to the magnetic pole allow to recognize four main structural zones (Fig. 7b): (red) located south of the area and characterized by predominant NE-SW and NW-SE lineaments; central, E-W elongated zone (yellow), with predominant NNE-SSW lineaments; northern zone (green) with predominant NE-SW and NW-SE lineaments and a N-S zone

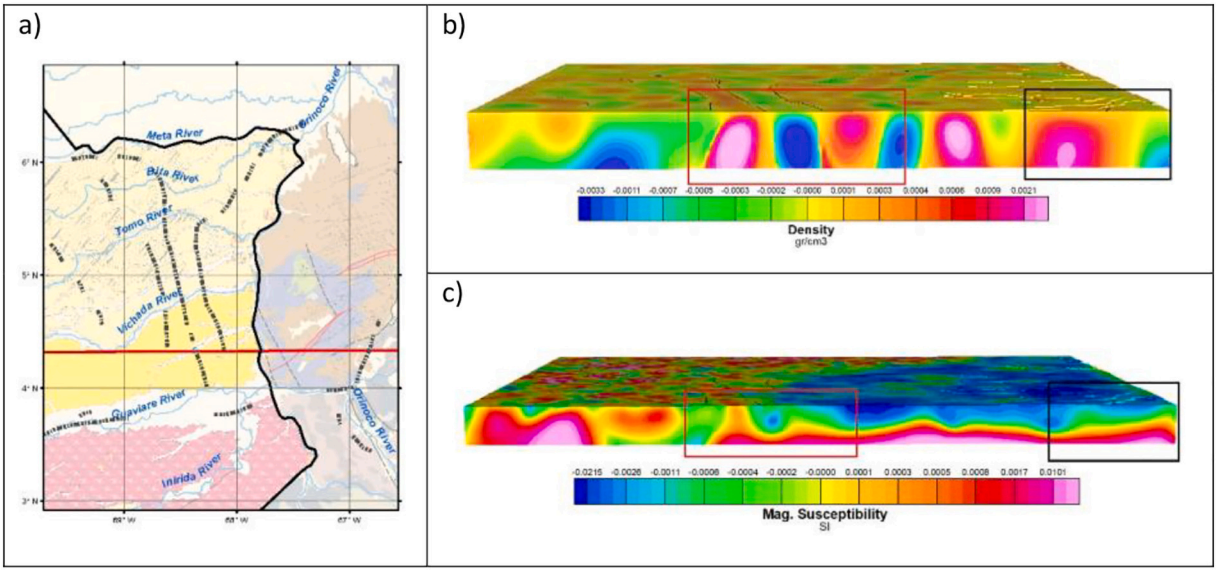

Fig. 14. Cross section along W-E profile (a, red line) of the density (b) and magnetic susceptibility (c) models. Red and black squares mark the relation of the models with the boundaries interpreted (black lines). (For interpretation of the references to colour in this figure legend, the reader is referred to the web version of this article.)

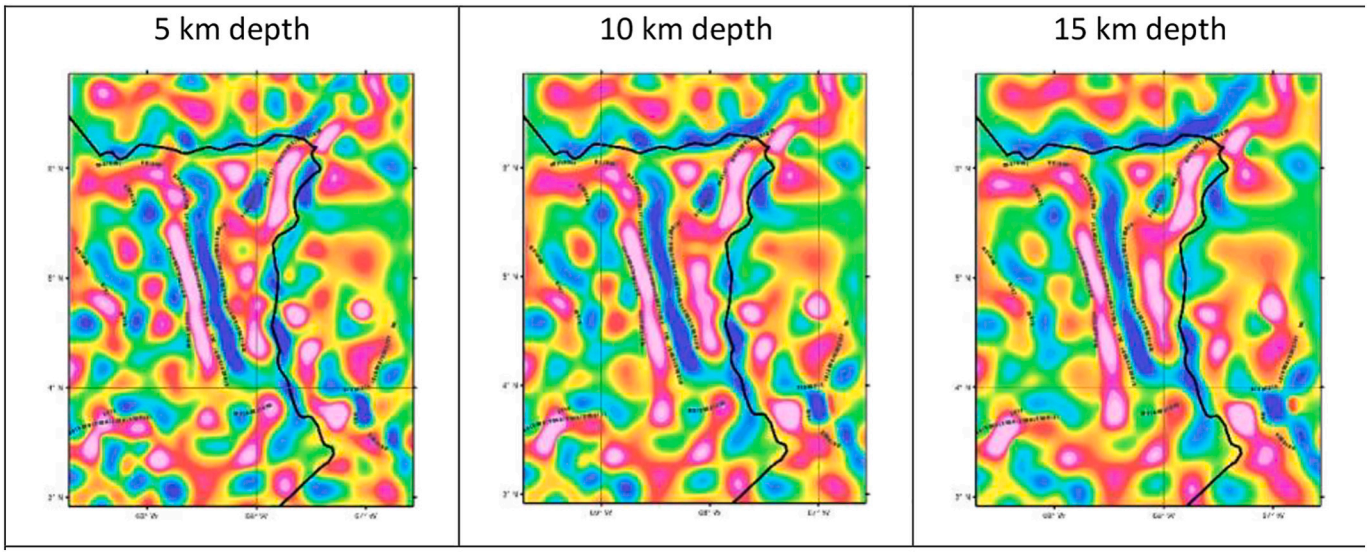

Fig. 15. Depth slices of the density model of Fig. 5b.

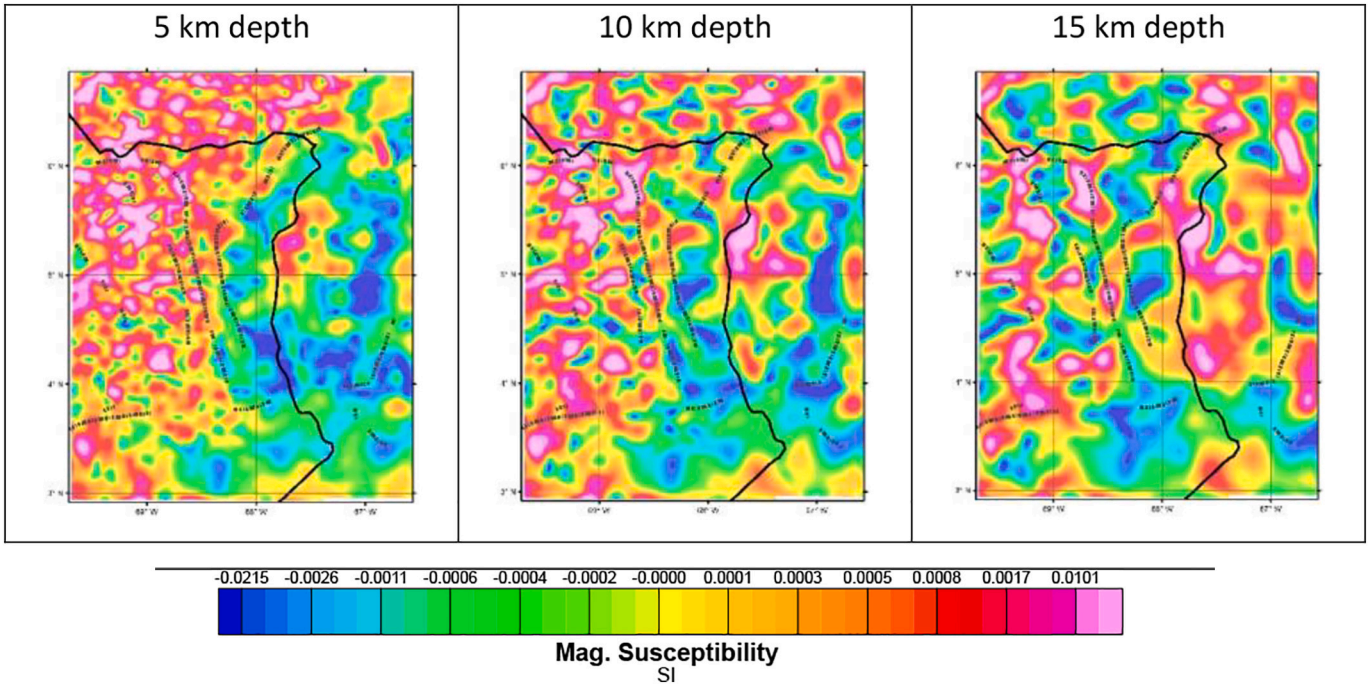

Fig. 16. Depth slices of the magnetic susceptibility model of Fig. 15c.

(blue) that cuts the green and yellow zones.

Multiscale edge detection ("worming") applied to gravity and magnetic data show deep crustal penetrating discontinuities that are closely related to and delimitate the structural zones and can represent geotectonic limits. The most remarkable are the nearly N-S edges related with a structural zone that were interpreted as the western limit of the Parguaza granite and an important high density/high magnetic susceptibility block that extend from 3.5 N to the north that are interpreted as a possible aborted rift or a suture zone by the collision of a volcanic arc. Also, the E-W edge interpreted along the Guaviare River (Fig. 13), that limit the expression of the N-S edges to the south and also controls the direction of the Guaviare River in Colombia and Ventuari and Orinoco rivers in Venezuela, were interpreted as a younger deformation event that affected the area. Examples of the tectonic significance of these edges can be seen in the SE of the area were the edges are correlated with the intrusive contact between the Parguaza Granite and basement rocks of the Cuchivero Group.

3D density and magnetic susceptibility (MVI) inversion models show that the higher density sources are located close to the edges interpreted. High magnetic susceptibility sources are more scattered but shows spatial and depth distribution closely related with the edges. This relation of high density and magnetic susceptibility distribution are coherent with the high gravity gradients reported for the boundaries of the Ventuari-Tapajós province in Brazil and also strong density and magnetic susceptibility variations that separate major tectonic events in the Gawler Craton in Australia. It must be noted that the interpreted contacts of the Parguaza Granite with basement rocks of Cuchivero/Mitú Groups are characterized by strong density contrasts but without magnetic susceptibility variations.

The NNW-SSE edge located at the SE of the area parallel to the

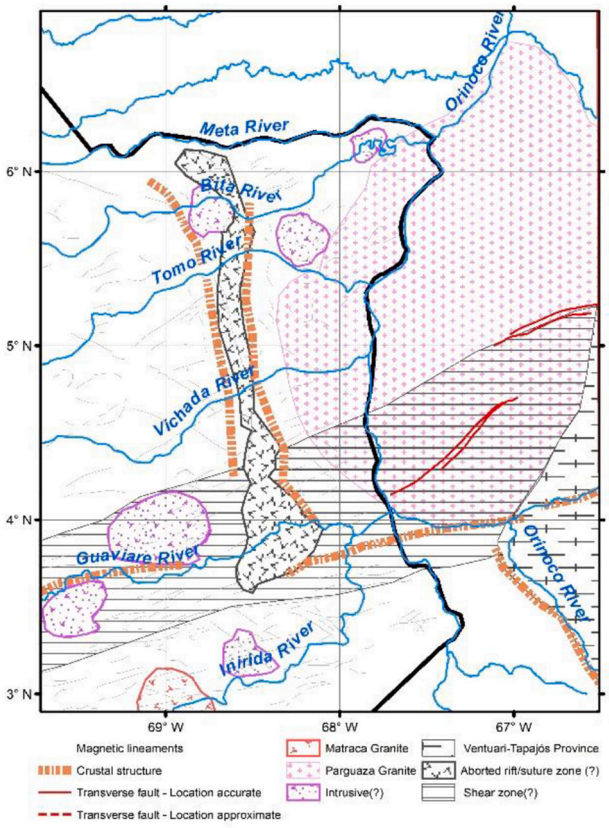

Fig. 17. Sketch map with main features interpreted in the present study and transverse faults.
Modified from Hackley et al., 2005.

Atabapo and Orinoco rivers in Venezuela can be interpreted as an evidence of the limit between the Ventuari Tapajos and Rionegro-Juruena geochronological provinces of Tassinari and Macambira (1999) but located to the east of the actual limit. Also, this edge can reflect the expression of the Atabapo Belt defined by Cordani et al., 2016b.

The vergence of the W-E shear zone interpreted along the Guaviare-Orinoco-Ventuari rivers is difficult to define from geophysical data only. Regional 1:100.000 maps of the SGC report a left-lateral displacement with normal component in NEE-SWW faults that also control the main drainages of the area, but the deep penetrating geophysical anomalies and edges interpreted for the present study suggest a right-lateral displacement that are reflected in the apparent tectonic control of the Orinoco, Guaviare and Ventuari rivers. On the other hand, the intrusion of the Parguaza Granite can also be responsible of these deep structural features or maybe this pre-existing weakness zone allowed the emplacement of the anorogenic intrusive body.

Interpretation of geophysical datasets with available geological information allow to identify and delineate major structural and tectonic features within the crystalline rocks of the Amazonian Craton (Fig. 17) that will help to improve the current structural/tectonic models for this area.

Further geological, structural, and geochronological investigations should be made to define more specifically the geotectonic processes that modelled the Amazonian Craton in the study area, but the structural framework interpreted in the present study provide new information that helps to prioritize areas of interest.

Declaration of Competing Interest

None.

Acknowledgement

The authors want to acknowledge the Departamento de Geociencias of the Universidad Nacional de Colombia and the Servicio Geológico Colombiano (Geological Survey of Colombia) for the support and collaboration in the present study as a part of the PhD in geosciences thesis of the first author. We also would like to thank Dr. Colin Reeves and other anonymous reviewer for their suggestions and recommendations that helped improve this contribution.

Appendix A. Supplementary data

Supplementary data to this article can be found online at https://doi.org/10.1016/j.tecto.2020.228705.

References

Alfonso, M., Herrera, J., Alzate, L., Arciniegas, E., Casas, R., Duarte, P., Marín, E., Méndez, C., Montaña, J., 2014. Memoria Explicativa de la Plancha 220 Río Tuparro. Servicio Geológico Colombiano, Bogotá (222 pp.).
Allaby, M., 2013. A Dictionary of Geology & Earth Sciences. Oxford University Press, Oxford, UK.
Arminio, J., Yoris, F., Quijada, C., Lugo, J., Shaw, D., Keegan, J., Marshall, J., 2013. Evidence for Precambrian Stratigraphy in Graben Basins below the Eastern Llanos Foreland, Colombia. Search and Discovery Article #50874.
Baines, G., Giles, D., Betts, P., Backe, G., 2009. Geophysically imaging Paleoproterozoic terrane boundaries in the unexposed northern Gawler Craton, Marla region. In: ASEG Extended abstracts – 20th Geophysical Conference, pp. 1–5.
Baines, G., Giles, D., Betts, P., 2010. 3D Geophysical modelling of the northern Gawler Craton, South Australia. Geosci. Australia Rec. 39, 95–107.
Baranov, V., 1964. Numerical calculation of the formula of reduction to the magnetic pole. Geophysics XXIX (1), 61–79.
Barrios, F., Cordani, U., Kawashita, K., 1985. Caracterización geocronológica del Territorio Federal de Amazonas, Venezuela. In: Memorias VI Congreso Geológico Venezolano. Tomo III, pp. 1432–1480.
Bird, D., 2001. Shear margins: Continent-ocean transform and fracture zone boundaries. Lead. Edge 2001, 150–159.
Blakely, R., Simpson, R., 1986. Approximating edges of source bodies from magnetic or gravity anomalies. Geophysics I (7), 1494–1498.
Bonilla, A., 2019. Origen y evolución de los granitoides proterozoicos del oriente colombiano, noroeste del Cratón Amazónico. Tesis de Doctorado en Geociencias. Universidad Nacional de Colombia, Facultad de Ciencias, Departamento de Geociencias, Bogotá, Colombia.
Bonilla, A., Frantz, J.C., Charão-Marques, J., Cramer, T., Franco, J.A., Amaya, Z., 2016. Magmatismo rapakivi en la cuenca media del río Inírida, departamento de Guainía, Colombia. Bol. Geol. 38 (1), 17–32.
Brito, B., 2011. The Paleoproterozoic in the South American continent: Diversity in the geologic time. J. S. Am. Earth Sci. 32, 270–286.
Bruneton, P., Pallard, B., Duselier, E., Varney, E., Bogotá, J., Rodríguez, E., Martín, E., 1983. Contribución a la geología del oriente de las comisarías del Vichada y del Guainía (Colombia). Geol. Norand. (6), 3–12.
Cardozo, A., Cubides, J., Zárate, A., Melo, L., 2009. Memoria explicativa de las planchas 162, 162 bis, 182 y 182 bis Puerto Carreño. Instituto Colombiano de Geología y Minería- INGEOMINAS (107 pp.).
Cediel, F., 2019. Phanerozoic orogens of northwestern South America: cordilleran-type orogens. Taphrogenic tectonics. The maracaibo orogenic float. The Chocó-Panamá Indenter. In: Cediel, F., Shaw, R. (Eds.), Geology and Tectonics of Northwestern South America. The Pacific-Caribbean-Andean Junction. Springer, Switzerland, pp. 3–95.
Celada, C., Garzón, M., Gómez, E., Khurama, S., López, J., Mora, M., Navas, O., Pérez, R., Vargas, O., Westerhof, A., 2006. Potencial de recursos minerales en el Oriente colombiano: compilación y análisis de la información geológica disponible fase 0 versión 1.0. Ingeominas (233 pp.).
Cordani, U., Ramos, V., Fraga, L., Cegarra, M., Delgado, I., De Souza, K., Gomes, F., Schobenhaus, C., (2016a). Explanatory Notes: Tectonic Map of South America, Second Edition scale 1:5 000 000. CGMW.
Cordani, H., Sato, K., Sproessner, W., Santos, F., 2016b. U-Pb zircon ages of rocks from the Amazonas Territory of Colombia and their bearing on the tectonic history of the NW sector of the Amazonian Craton. Brazil. J. Geol. 46, 5–35.
Crawford, B., Betts, P., Ailleres, L., 2010. A potential field approach to defining major lithospheric structures along the margin of the West Australian Craton. In: ASEG 2010. Sydney, Australia.
De Boorder, H., 1981. Structural-geological interpretation of SLAR imagery of the Colombian Amazones. Trans. Inst. Min. Metall. 90, B145–B152.
De Boorder, H., 2019. The La Trampa wedge (SE Colombia) revisited. In: 11th Inter Guiana Geological Conference, Paramaribo, 19–20 February 2019.
De Castro, D., Phillips, J., Fuck, R., Vidotti, R., Bezerra, F., 2013. Using airborne gravity and magnetic data to recognize crustal domains concealed un-derneath the Parnaíba basin. In: 13th International Congress of the Brazilian Geophysical Society, Brazil, August 26–29, 2013.

De la Espriella, R., Flórez, R., Galvis, J., González, C.F., Mariño, J., Pinto, H., 1990. Geología regional del Norte de la Comisaría del Vichada. Geol. Colombia. 17, 93–106.
Dentith, M., Mudge, S., 2014. Geophysics for the Mineral Exploration Geoscientist. Cambridge University Press (ISBN 9780521809511).
Ellis, R., Wet, B., Macleod, I., 2012. Inversion of Magnetic Data from Remanent and Induced Sources. ASEG Extended Abstracts, 1-4. https://doi.org/10.1071/ASEG2012ab117.
Ferreira, M., Dantas, E., Nogueira, M., Vitória, R., 2011. Aeromagnetometria na Caracterização do rifte intracontinental na Faixa Paraguai. In: Twelfth International Congress of the Brazilian Geophysical Society, pp. 709–714.
FitzGerald, D., Milligan, P., 2013. Defining a Deep Fault Network for Australia, Using 3D "worming". SEG Annual Meeting. Houston (TX), USA, pp. 1126–1130.
Förste, C., Bruinsma, S., Abrikosov, O., Lemoine, J., Marty, J., Flechtner, F., Balmino, G., Barthelmes, F., Biancale, R., 2014. EIGEN-6C4: the latest combined global gravity field model including GOCE data up to degree and order 2190 of GFZ Potsdam and GRGS Toulouse. In: GFZ Data Services. https://doi.org/10.5880/icgem.2015.1.
Galvis, J., Huguett, A., Ruge, P., De Boorder, H., (1979). Mapa Geológico de la Amazonia Colombiana. Scale 1:500.000. Proyecto Radargramétrico del Amazonas. Bogotá.
Geng, M., Welford, J., Farquharson, C., Hu, X., 2019. Gravity modeling for crustal-scale models of rifted continental margins using a constrained 3D inversion method. Geophysics 84 (4), G25–G39. July–August 2019.
Gómez, J., Montes, N., Nivia, A., Diederix, H., 2015a. Geological Map of Colombia 1: 1.000.000. Servicio Geológico Colombiano, Bogotá.
Gómez, J., Montes, N., Nivia, A., Diederix, H., 2015b. Atlas Geológico de Colombia 2015. Escala 1:500 000. Servicio Geológico Colombiano, Bogotá (compiladores).
Gómez, J., Schobbenhaus, C., Montes, N., 2019. Geological Map of South America 2019. Scale 1:5 000 000. Commission for the Geological Map of the World (CGMW), Colombian Geological Survey and Geological Survey of Brazil, Paris.
González, C., Pinto, H., 1990. Petrografía del Granito de Parguaza y otras rocas precámbricas en el Oriente de Colombia. Geol. Colomb. 17, 107–121.
González, H., Escobar, A., Cáceres, C., Correa, R., Ayala, L., Fernández, F., Villada, I., López, F., 2014. Plancha 219 – Parque nacional natural El Tuparro: Memoria explicative. Servicio Geológico Colombiano (113 pp.).
González, W., Sigismondi, M., Graterol, V., Jácome, M., Izarra, C., 2017. Magnetic characterization and signature of the basement of Eastern Venezuela: Espino Graben. In: SEG International Exposition and 87th Annual Meeting. Houston, pp. 1589–1864.
Graterol, V., 2009. Levantamiento Aerogravimétrico y Aeromagnético de los sectores Norte y Oriental de la Cuenca de los llanos Orientales, Colombia Contrato No.034-2008. Informe final de Interpretación. Agencia Nacional de Hidrocarburos (ANH) (51 pp.).
Graterol, V., Vargas, A., 2010. Mapa de Anomalía de Intensidad Magnética Total y de Intensidad Magnética Total Reducida al Polo de la República de Colombia y Mapa de Anomalía de Bouguer total de la República de Colombia. Agencia Nacional de Hidrocarburos (ANH).
Gusmao, R., Freitas, J., 2014. Interpretação geofísica dos principais domínios tectônicos brasileiros. In: Serviço Geológico do Brasil (CPRM), Metalogênese das províncias tectônicas brasileiras. Belo Horizonte, pp. 21–40.
Gusmao, R., De Medeiros, W., Pessoa, A., 2005. Expressão gravimétrica e aeromagnética dos compartimentos e limites tectônicos da Província Borborema, Nordeste do Brasil. In: 9th International Congress of the Brazilian Geophysical Society, Brazil, September 11–14, 2005.
Hackley, P., Urbani, F., Karlsen, A., Garrity, C., 2005. Geologic shaded relief map of Venezuela. In: USGS Open-file report 2005-1038.
Heath, P., Dhu, T., Reed, G., Fairclough, M., 2009. Geophysical modelling of the Gawler Craton, SA - interpreting geophysics with geology. In: ASEG Extended abstracts – 20th Geophysical Conference.
Holden, D., Archibald, N., Boschetti, F., Jessell, M., 2000. Inferring geological structures using wavelet-based multiscale edge analysis and forward models. Explor. Geophys. 31, 67–71.
Hornby, P., Boschetti, F., Horowitz, F., 1999. Analysis of potential field data in the wavelet domain. Geophys. J. Int. 137, 175–196.
Horowitz, F., Strykowski, G., Boschetti, F., Hornby, P., Archibald, N., Holden, D., Ketelaar, P., Woodcock, R., 2000. Earthworms; "Multiscale" Edges in the EGM96 Global Gravity Field. SEG Expanded Abstracts. Alberta, Canadá.
Ibáñez-Mejía, M., Ruiz, J., Valencia, V., Cardona, A., Gehrels, G., Mora, A., 2011. The Putumayo Orogen of Amazonia and its implications for Rodinia reconstructions: new U–Pb geochronological insights into the Proterozoic tectonic evolution of northwestern South America. Precambrian Res. 191, 58–77.
Isles, D., Rankin, L., 2013. Geological Interpretation of Aeromagnetic Data. Australian Society of Exploration Geophysicist (ISBN 0-521-33938-3).
Jackson, D., 1972. Interpretation of inaccurate, insufficient and inconsistent data. Geophys. J. R. Astr. Soc. 28, 97–109.
Kohanpour, F., Lindsay, M., Occhipinti, S., Gorczyyk, W. (2018). Structural controls on proterozoic nickel and gold mineral systems identified from geodynamic modelling and geophysical interpretation, east Kimberley, Western Australia. Ore Geol. Rev. 95 (2018), pp 552–568. Elsevier.
Kroonemberg, S., 2019. The proterozoic basement of the Western Guiana shield and the Northern Andes. In: Cediel, F., Shaw, R. (Eds.), Geology and Tectonics of Northwestern South America. The Pacific-Caribbean-Andean Junction. Springer, Switzerland, pp. 115–192.
Kroonenberg, S., Reeves, C., 2012. Geology and petroleum potential, Vaupés-Amazonas Basin, Colombia. In: Cediel, F. (Ed.), Petroleum Geology of Colombia, 15. Universidad EAFIT, Medellín (92 pp.).
López, J., Mora, B., Jiménez, D., Khurama, S., Marín, E., Obando, G., Páez, T., Carrillo, L., Bernal, V., Celada, C., 2010. Cartografía geológica y muestreo geoquímico de las Planchas 297 – Puerto Inírida, 297 Bis – Merey Y 277 Bis – Amanaven. Departamento del Guainia, Ingeominas, Bogotá (158 pp.).
MacLeod, I., Ellis, R., 2013. Magnetic Vector Inversion, a simple approach to the challenge of varying direction of rock magnetization. In: ASEG-PESA 23rd International Geophysical Conference and Exhibition. Melbourne, Australia.
Meyer, B., Saltus, R., Chulliat, A., 2017. EMAG2: Earth Magnetic Anomaly Grid (2-arc-minute Resolution) Version 3. National Centers for Environmental Information, NOAA. https://doi.org/10.7289/V5H70CVX. Model.
Moyano, I., Lara, N., Ospina, D., Salamanca, A., Arias, H., Gómez, E., Puentes, M., Rojas, O., 2018. Mapa de anomalías Geofísicas de Colombia para Recursos Minerales, Versión 2018. Servicio Geológico Colombiano, Bogotá.
Ochoa, A., Ríos, P., Cardozo, A., Cubides, J., Giraldo, D., Rincón, H., Mendivelso, D., 2012. Cartografia geologica y muestreo geoquimico de las planchas 159, 160, 161, 179, 180 y 181 Puerto Carreño, Vichada. Memoria explicativa. Servicio Geológico Colombiano, Bogotá (127 pp.).
Ochoa, A., Ríos, P., Oviedo, J., Cardozo, A., Cubides, J., 2014. "Cartografía geológica y muestreo geoquimico de las planchas 237 y 256 Departamento de Vichada": Memoria explicativa. Memoria explicativa. Servicio Geológico Colombiano, Bogotá (85 pp.).
Park, Y., Rim, H., Lim, M., Hong, Y., Jeon, T., 2013. Magnetic characteristics of tectonic provinces of Korea. In: Proceedings of the 11th SEGJ International Symposium, Yokohama, Japan, pp. 146–149.
Parker, R., 1977. Understanding inverse theory. Annu. Rev. Earth Planet. Sci. 5, 35–64.
Rodríguez, G., Sepúlveda, J., Ortiz, F., Ramírez, C., Ramos, K., Bermúdez, J., Sierra, M., 2010. Mapa Geológico Plancha 443 Mitú – Vaupés. Ingeominas.
Santos, J., Hartmann, L., Gaudette, H., Groves, D., Mcnaughton, N., Fletcher, I., 2000. A new understanding of the provinces of the Amazon Craton based on integration of field mapping and U-Pb and Sm-Nd geochronology. Gondwana Res. 3 (4), 453–488.
Soares, L., Da Costa, M., 2013. New concepts of continental passive margins: gravity and magnetic interpretation in Western Iberia. In: Thirteenth International Congress of the Brazilian Geophysical Society, Rio de Janeiro, Brazil, pp. 344–349.
Tassinari, C., Macambira, M., 1999. Geological provinces of the Amazonían Craton. Episodes 22, 173–182.
VanDecar, J., Snieder, R., 1994. Obtaining smooth solutions to large, linear, inverse problems. Geophysics 59 (5), 818–829.
Yan, J., Lü, Q., Deng, Z., Meng, G., Liu, Y., Zhao, J., 2011. Gravity and magnetic multi-scale edge detection and its application on tectonic framework research of the lower and middle reaches of the Yangtze River Metallogenic Belt, China. In: GEM Beijing 2011: International Workshop on Gravity, Electrical & Magnetic Methods and Their Applications Beijing, China. October 10-13, 2011.